Published in final edited form as:
Prog Biophys Mol Biol. 2011 May ; 105(3): 247–257. doi:10.1016/j.pbiomolbio.2010.11.001.

Chaos in the Genesis and Maintenance of Cardiac Arrhythmias

Zhilin Qu
Department of Medicine (Cardiology), David Geffen School of Medicine at University of California, Los Angeles, California 90095

Abstract

Dynamical chaos, an irregular behavior of deterministic systems, has been widely shown in nature. It also has been demonstrated in cardiac myocytes in many studies, including rapid pacing induced irregular beat-to-beat action potential alterations and slow pacing induced irregular early afterdepolarizations, etc. Here we review the roles of chaos in the genesis of cardiac arrhythmias, the transition to ventricular fibrillation, and the spontaneous termination of fibrillation, based on evidence from computer simulation of mathematical models and experiments of animal models.

Keywords

Chaos; arrhythmias; reentry; fibrillation; spiral wave; synchronization

1. Introduction

Ventricular fibrillation (VF) is the leading cause of sudden cardiac death, the No.1 killer in the industrialized countries (Lopshire and Zipes, 2006; Zipes and Wellens, 1998). Understanding the underlying mechanisms is undoubtedly necessary for developing effective therapies.

The occurrence of cardiac arrhythmias depends on two necessary components: triggers and tissue substrates. Arrhythmias can be maintained by one or more foci, or by reentry, or by a mixture of both (Janse, 2007; Waldo and Wit, 1993; Wu et al., 2004). Reentry can be initiated when a trigger, such as a premature ventricular complex (PVC), encounters a region of prolonged refractory period and/or slowed conduction (Chen et al., 1988; Winfree, 1983). Tissue substrates refer to heterogeneous spatial properties (e.g., refractory periods, intracellular calcium transients, or conduction properties, etc) that allow foci or reentry to form locally. Traditionally, both triggers and substrates are considered to be promoted by pre-existing tissue heterogeneities, the intrinsic electrophysiological and structural differences in space which are often exacerbated in diseased hearts (Akar and Rosenbaum, 2003; El-Sherif et al., 1991; Janse and Wit, 1989; Restivo et al., 1990). PVCs occur occasionally in normal hearts and much more frequently in diseased hearts, but most of them are benign. Only few of them may result in lethal arrhythmias (Glass, 2005; Lerma et al., 2007), raising a question: why are those PVCs so special? An answer to this question is that

Correspondence to: Zhilin Qu, PhD, Department of Medicine (Cardiology), David Geffen School of Medicine at UCLA, A2-237 CHS, 650 Charles E. Young Drive South, Los Angeles, CA 90095, Tel: 310-794-6050, Fax: 310-206-9133, zqu@mednet.ucla.edu.

either the triggers or the substrates or both are dynamic, and only when a proper trigger encounters a proper substrate, reentry forms. Many dynamical factors that lead to reentry substrates have been identified (Otani et al., 2005; Qu and Weiss, 2006; Weiss et al., 2006; Weiss et al., 2005). Examples are electrical restitution and intracellular calcium cycling causing spatially discordant repolarization alternans (Cao et al., 1999; Pastore et al., 1999; Qu et al., 2000a; Weiss et al., 2006) and PVCs causing repolarization gradients due to electrical restitution (Akar et al., 2002; Antzelevitch et al., 1991; Comtois et al., 2005; Laurita et al., 1996; Otani, 2007; Qu et al., 2006a; Qu et al., 2006b; Restivo et al., 2004). In recent studies (Sato et al., 2009; Xie et al., 2007), we identified a novel dynamics, chaos and chaos synchronization, which can cause both arrhythmia triggers and substrates to occur dynamically in both time and space.

Once a reentry or a focus forms in cardiac tissue, it may stay intact to manifest ventricular tachycardia (VT). But it may decay into multiple wavelets, manifesting VF. Two major hypotheses of VF have been proposed and validated experimentally in animal models: the mother rotor hypothesis and the multiple wavelets hypothesis. In mother rotor hypothesis (Chen et al., 2003; Jalife et al., 2002), pre-existing heterogeneities (dispersion of refractoriness) cause fibrillatory conduction block of waves from a stable high frequency focal source or a rotor, accounting for the multiple wavelets observed during fibrillation. In the multiple wavelet hypothesis (Moe, 1982; Moe et al., 1964), however, pre-existing heterogeneities are not necessary, since fibrillation is maintained by spontaneous spiral wave breakup due to dynamical instabilities. Modeling studies (Bar and Eiswirth, 1993; Fenton et al., 2002; Panfilov and Holden, 1991; Qu et al., 2000b; Qu et al., 2000c) have shown that spiral wave breakup is a transition to spatiotemporal chaos.

Arrhythmias can terminate spontaneously, frequently in atria or small hearts but only occasionally in large ventricles (Clayton et al., 1993; Wijffels et al., 1995). Anti-arrhythmic drugs can terminate ventricular fibrillation and are fairly effective at terminating atrial fibrillation (Manoach et al., 1987; Naccarelli et al., 2003). The formation and maintenance of arrhythmias depends on tissue size and form, as observed in 1914 by Garrey (Garrey, 1914), the earliest experimental basis for the well-known “critical mass hypothesis.” Based on this hypothesis, prolonging the refractory period (thus wavelength) effectively reduces the tissue size, which can promote termination of arrhythmias. Using computer simulations (Qu, 2006; Qu and Weiss, 2005), however, we showed that besides wavelength, dynamical instabilities, such as chaos, played an important role in terminating arrhythmias.

In this article, we review the roles of chaos in the genesis of arrhythmias, the degeneration of VT to VF, and the termination of VF, based on evidence from computer simulation of mathematical models and experiments of animal models.

2. Dynamical chaos

Chaos is a complicated behavior arising from deterministic nonlinear systems under certain parameter settings, which looks erratic and random. It can be generated from very simple systems. Such a text book example is the so-called Logistic map, a difference equation describing population dynamics of ecosystems (May, 1976), i.e.,

$$x_{n+1}=f(x_n)=\alpha x_n-\beta x_n^2 \quad (1)$$

where x_n is the population of the present generation, x_{n+1} is the population of the next generation, α and β are the two parameters determining the behaviors of the system. The function $f(x_n)$ in Eq.1 includes two terms: the first term is the total number of births and the

second term is the total number of deaths. In general, the competition between births and deaths settles the system at an equilibrium state. However, this is not always the case due to the nonlinear term in Eq.1, and very complicated behaviors can emerge. To simplify the analysis of Eq.1, we assume β=α, then Eq.1 becomes:

$$x_{n+1}=f(x_n)=\alpha x_n(1-x_n) \quad (2)$$

which is the canonical form of the Logistic map (May, 1976; Strogatz, 2000). $f(x_n)$ in Eq.1 or Eq.2 is a parabolic function (Fig.1A). The equilibrium states of Eq.2 are the solutions of the equation $x_n=f(x_n)$, which are simply the intersections of the parabola and the diagonal line as shown in Fig.1A. The behaviors of Eq.2 are summarized in the bifurcation diagram shown in Fig.1B, in which the values of x_n versus the parameter α are plotted after the initial transients are dropped. When α<3, the non-zero equilibrium state is stable, and the system always approaches this equilibrium state with any initial conditions (Fig.1C). However, as α increases to be just bigger than 3, the equilibrium state becomes unstable (dashed line in Fig. 1B), a new type of behavior emerges, which exhibits a large-small-large-small alternating pattern (Fig.1D). As α increases further, more complex behaviors occur, and eventually x_n behaves in a non-periodic manner (Fig.1E), which is dynamical chaos.

Chaos is qualitatively different from the periodic behaviors, not only due to its erratic appearance but also due to its sensitivity to initial perturbations. For example, the two chaotic traces shown in Fig.1E are results from two different initial conditions: x_1=0.2 and x_1=0.20001. Although the initial difference is only 10^{-5}, it gets amplified after about 10 iterations to the macroscopic scale that makes the two iteration sequences to look completely different. This property is the hallmark of chaos: sensitive dependence on initial condition, also called the "butterfly effect", a metaphor was first used by Lorenz in one of his talks on weather dynamics entitled (Hilborn, 2004;Lorenz, 1994): "Does the flap of a butterfly's wings in Brazil set off a tornado in Texas?"

3. Cardiac chaos

Chaos has been shown in cardiac myocytes in many experimental (Chialvo et al., 1990a; Garfinkel et al., 1992; Guevara et al., 1981; Watanabe et al., 1995) and modeling (Chialvo et al., 1990b; Guevara and Glass, 1982; Lewis and Guevara, 1990; Qu et al., 2007) studies. Figure 2A shows a bifurcation diagram obtained from cardiac Purkinje fibers in experiments by Chialvo et al (Chialvo et al., 1990a), showing that as the basic or pacing cycle length (PCL) decreases, the action potential behaviors become more and more complex, including alternans (a *long-short-long-short* alternating pattern of action potential duration (APD)) and irregular dynamics (ID) (Fig.2B). Note that the bifurcation diagram obtained experimentally resembles the bifurcation diagram shown in Fig.1B. Indeed, the bifurcation in Fig.2A can be recapitulated using an iterated map as Eqs.1 and 2, formulated using the APD restitution curve (Franz et al., 1988; Goldhaber et al., 2005; Koller et al., 1998; Watanabe et al., 1995), i.e., the dependence of APD on its previous DI, as follows:

$$APD_{n+1}=f(DI_n)=f(PCL-APD_n) \quad (3)$$

where PCL is the pacing cycle length satisfying $PCL=APD_n+DI_n$. This type of iterated map was first used by Nolasco and Dahlen (Nolasco and Dahlen, 1968) 40 years ago to investigate the mechanism of alternans observed in strips of in vitro frog ventricular muscle subjected to electrical stimulation. They showed that when the slope of the APD restitution curve exceeded 1, periodic beating gave way to APD alternans. Later studies (Chialvo et al., 1990a; Guevara et al., 1984; Hastings et al., 2000; Lewis and Guevara, 1990; Qu, 2004; Qu

et al., 2007; Xie et al., 2007) showed that, in addition to alternans, more complex dynamics could be elicited by periodic pacing. Fig.2C shows a bifurcation diagram obtained by iterating Eq.3 with $f(DI_n) = 220 - 180e^{-DI_n/60}$, in which the bifurcation sequence is 1:1 → 2:2 → 2:1 → 4:2 → ID (chaos) → 4:1 → 8:2 → ID (chaos) as PCL decreases. This is very similar to the bifurcation sequence obtained in experiments in cardiac Purkinje fibers shown in Fig.2A, which is 1:1 → 2:2 → 2:1 → 4:2 → 3:1 → 6:2 → 4:1 → 8:2 → ID. Similar bifurcation sequences have been observed in simulations of action potential models (Fig.2D) (Hastings et al., 2000; Lewis and Guevara, 1990; Qu, 2004; Xie et al., 2007). Other bifurcation sequences and mechanisms of chaos in cardiac myocytes have also been demonstrated, such as the period-doubling bifurcation route to chaos (Guevara and Glass, 1982; Watanabe et al., 1995).

In recent studies (Sato et al., 2009; Tran et al., 2009), we have demonstrated another type of chaos in cardiac myocytes, i.e., chaotic early afterdepolarizations (EADs). Irregular behavior of EADs has been widely observed in single myocytes in experimental studies (Gilmour and Moise, 1996; Li et al., 2002; Song et al., 1992), which has been generally attributed to random fluctuations of underlying ion channels (Tanskanen et al., 2005). Using both computational simulations and experiments of isolated myocytes, we have shown that this irregularity is dynamical chaos. Figure 3 compares the experimental recordings of voltage and the APD bifurcation diagram (Fig.3A) with those from the computer simulations (Fig. 3B). The bifurcation diagrams are similar, i.e., irregular behaviors of EADs only occur at the intermediate PCLs, at either slow or rapid pacing, the action potentials are regular. Since the computational model (Mahajan et al., 2008; Sato et al., 2009) is completely deterministic, no random fluctuations exist, the irregular behavior is simply dynamical chaos. However, random fluctuations in ion channels or heart rates, which naturally exist in the heart, may play important roles for the irregularly appearing EADs (Kim et al., 2009; Sato et al., 2010; Tanskanen et al., 2005).

4. Chaos synchronization and cardiac arrhythmogenesis

Chaos synchronization

Due to the butterfly effect, two uncoupled identical chaotic systems look completely different and are uncorrelated (Fig.1E). However, when the two chaotic systems are coupled, they can be completely synchronized though the individual ones are still chaotic, which is called chaos synchronization (Pecora and Carroll, 1990;Pecora et al., 1997). Figure 4 shows chaos synchronization in two identical Logistic maps coupled diffusively, i.e.,

$$\begin{aligned} x_{n+1} &= 4x_n(1 - x_n) + \varepsilon(y_n - x_n) \\ y_{n+1} &= 4y_n(1 - y_n) + \varepsilon(x_n - y_n) \end{aligned} \tag{4}$$

where ε is the coupling strength. When ε=0, the two systems are uncoupled and independent, and behave completely different even though the initial conditions are just slightly different (see Fig.1E). When the coupling is weak (ε=0.2), the two systems still go apart and become uncorrelated (Fig.4A). However, when the coupling is strong (ε=0.3), the two systems synchronize even though the initial conditions differ largely (Fig.4B). Note that after synchronization, the coupled system is still chaotic. This phenomenon can be generally understood as follows. The diffusive coupling tends to reduce the difference between the two systems, however, the “butterfly effect” of chaos tends to amplify the difference. Therefore, if the coupling is strong enough, the smoothing effect of coupling wins over the amplifying effect of chaos, the two systems maintain synchronized, otherwise synchronization fails.

Chaos synchronization in cardiac tissue and the genesis of cardiac arrhythmias

Cardiac myocytes are diffusively coupled through gap junction conductance. When the myocytes are paced simultaneously with periodic stimulation, they are always synchronized when the action potential dynamics are not chaotic (Wang et al., 2007; Xie et al., 2007). When they are driven into chaos, they can be either synchronized or dyssynchronized, depending on the gap junction conductance or tissue size (Sato et al., 2009; Xie et al., 2007). For a fixed gap junction conductance, synchronization can only occur when the number of cells or tissue size is below a critical value (Fig.5A). When the tissue size exceeds the critical value, synchronization cannot be maintained, leading to regions of long action potential bordering with regions of short action potential (Fig.5B). On the other hand, for a fixed tissue size, if the gap junction conductance is large enough, all the myocytes can keep synchronized while the action potential dynamics of the individual myocytes maintain chaotic. If the gap junction conductance is small, the myocytes become asynchronous.

When complete synchronization fails due to a large tissue size or a weak gap junction coupling, the consequence is that large gradients of refractoriness develop, irrespective to the causes of chaos. In other words, dispersion of refractoriness occurs for either rapid pacing-induced chaos (Fig.5B) or slow pacing-induced EAD chaos (Figs.5C and D). In 2D and 3D tissue, islands of long APD neighboring with short APD regions develop.

In the case of rapid pacing induced chaos, reentry can be induced in homogeneous tissue without requiring pre-existing heterogeneities and additional triggers (Fig.6) (Xie et al., 2007). In the case of slow pacing-induced EAD chaos, both triggers and substrates are simultaneously generated by the same dynamical mechanism, and reentry develops spontaneously without any requirement for pre-existing tissue heterogeneities (Sato et al., 2009).

When the magnitude of EADs is small, they cannot propagate in tissue, so that partial regional chaos synchronization only results in dispersion of refractoriness. When the EAD magnitude is large enough so that it can propagate, partial regional synchronization of chaos gives rise to localized EADs which propagate as PVCs into adjacent recovered regions. This is illustrated in Fig.7A, in which a paced 1D cable develops a localized PVC near the middle of the cable after the last pacing beat, which propagates towards both ends of the cable. If the homogeneous cable is longer, multiple PVCs can form in the cable, maintaining the electrical activities in the cable for a longer time after the stimulation is stopped (Fig.7B). The duration of the activities depends on the length of the cable, and can be prolonged if the cable length is further increased. In a homogeneous 2D tissue (Fig.7C), multiple foci develop spontaneously after several pacing beats, varying both in time and location, similar to the 1D cable. The mechanism is as follows: an EAD-triggered PVC due to partial regional chaos synchronization at one location propagates into recovered cells in an adjacent region, where it induces a new EAD-mediated PVC in that region. This new PVC propagates into less recovered adjacent tissue, generating an EAD-mediated PVC in this new region, and so forth. This leads to spontaneous formation of multiple foci which vary dynamically in time and space. This same phenomenon can be simulated in an anatomical model of rabbit ventricle. Two episodes of multiple shifting foci are shown in Fig.8A, manifesting as polymorphic VT on the pseudo-electrocardiogram (Fig.8B). Similar behaviors have been shown in intact rabbit hearts exposed to 0.2–1 mM H_2O_2 (Figs.8C and D), and in drug-induced long QT models (Asano et al., 1997;Choi et al., 2002).

5. Spatiotemporal chaos due to spiral wave breakup resembling VF

As shown in experiments (Chen et al., 1988; Hwang et al., 1996), once a single or a figure-of-eight reentry is induced, it usually lasts for a few beats and then degenerates into multiple

wavelets VF. Computer simulation studies (Qu et al., 1999; Qu et al., 2000c) have shown that APD restitution is a critical parameter that controls the stability of the spiral wave reentry. Namely, when APD restitution is flat, the spiral wave is stable (Fig.9A), and as APD restitution becomes steeper, the spiral wave meanders yet remains intact (Figs.9B and C). These spiral wave behaviors resemble either monomorphic or polymorphic VT (Qu and Garfinkel, 2004). When APD restitution becomes even steeper, the spiral wave becomes unstable and breaks up spontaneously into multiple small reentrant waves (Fig.9D), which resembles fibrillation. Note that the computer simulations shown in Fig.9 are performed in completely homogeneous tissue models, yet a large dispersion of refractoriness is resulted purely from the dynamical instability of the spiral waves. In this case, spiral waves are constantly created and disappear in an irregular or chaotic manner. The transitions from stable spiral wave to meandering spiral wave, and to spiral wave breakup are transitions from a periodic behavior to a quasiperiodic behavior, and to chaos (Fig.9E). The genesis of wavebreaks and irregular dynamics is similar to the n:m block and irregular dynamics in the isolated cell as shown in Fig.2. Many recent experimental studies (Garfinkel et al., 2000; Riccio et al., 1999; Wu et al., 2002) have shown that pharmacological agents that reduce the slope of APD restitution convert fibrillation into tachycardia, supporting the theory developed through computer modeling studies. Figure 10 shows an example of experiments by Wu el al (Wu et al., 2002), in which calcium channel blocker D600 is used to change APD restitution properties (Fig.10A) and converts VF to VT, and then VT to VF after washout (Fig.10B). VF is manifested by multiple reentrant wavelets (Fig.10C) and VT is manifested by a pair of stable spiral waves (Fig.10D).

6. Chaos in termination of arrhythmias

In hearts of large mammals, including humans, spontaneous termination of fibrillation occurs frequently in atria but only occasionally in the ventricles. Anti-arrhythmic drugs can terminate ventricular fibrillation and are fairly effective at terminating atrial fibrillation (Manoach et al., 1987; Naccarelli et al., 2003). To some extent, their antifibrillatory actions have been rationalized according to Garrey's "critical mass hypothesis" (Garrey, 1914) and Moe's "multiple wavelet hypothesis" (Moe, 1982; Moe et al., 1964). For example, Class IA and III anti-arrhythmic drugs prolong wavelength, so that the same size tissue can support fewer reentrant circuits, which may cause fibrillation to self-terminate. However, this mechanism has been challenged by experimental studies (Goy et al., 1985; Wijffels et al., 2000) which show that these drugs have limited effects on wavelength and refractory period. Using computer modeling (Qu, 2006; Qu and Weiss, 2005), we show that chaotic wave dynamics plays an important role in the termination of fibrillation. Although dynamical instabilities due to steep APD restitution promote wavebreaks and fibrillation, but it also enhances the probability of wave extinction by promoting wave meandering and collision with tissue borders, facilitating spontaneous termination of fibrillation (Fig.11A). The latter effect predominates as the dynamical instability or the steepness of the APD restitution increases, so that fibrillation is more likely to self-terminate in a finite size tissue (Fig.11 B and C). The likelihood of spontaneous termination of fibrillation decreases exponentially as tissue size increases (Fig.11D). In fact, anti-arrhythmic drugs, either Class IA or III, may terminate fibrillation through their effects on electrical restitution as well as wavelength, since the reverse-use dependence of potassium channel blockers prolongs APD at slow rates, but much less at fast rates, making APD restitution steeper. This steepening causes the reentrant waves to be more unstable, enhancing their probability of colliding with other waves or tissue borders and self-terminating. Promoting spiral wave instabilities by drug-induced steepening of APD restitution to terminate arrhythmias has been demonstrated in experimental studies (Amino et al., 2005; Banville and Gray, 2002; Yamazaki et al., 2007), agreeing with the theoretical predictions.

Chaos may also play an important role in termination of multi-focal polymorphic VT. As shown in Fig.7, when the tissue size is small (Fig.7A), only one focus forms which terminates spontaneously. As the tissue size becomes larger (Fig.7B), multiple foci occur. Since these foci occur and disappear chaotically, the multi-focal arrhythmias eventually terminate. This same mechanism may be responsible for the frequently observed spontaneous termination of polymorphic VT or Torsade de Pointes in clinical settings, especially in long QT syndromes.

Therefore, the dynamical wave instabilities due to spatiotemporal chaos can result in spontaneous termination of fibrillation, providing novel insight into the underlying mechanisms, which flourishes the traditional "critical mass hypothesis."

7. Concluding remarks

Cardiac arrhythmias are complex abnormal electrical wave activities in the heart, which are regulated by factors ranging from the molecular level to the whole heart. In this review, we summarized the effects of dynamical chaos on the genesis and maintenance of arrhythmias based on studies of computer simulation and animal experiments. The main point is that the factors that promote arrhythmias, such as dispersion of refractoriness, PVCs, focal excitations, and wavebreaks, can be produced in homogeneous tissue due to dynamical instabilities, namely dynamical chaos. But the same instabilities can also make arrhythmias terminate in finite-size tissue. Since this conclusion is based on computer modeling and animal experiments, a question arising is how these dynamics are related to arrhythmias and sudden cardiac death in human. Sudden cardiac death usually occurs in patients with coronary artery diseases but can also occur in patients with no symptoms and structurally normal hearts (Chugh et al., 2000; Lopshire and Zipes, 2006). In hearts with coronary artery diseases, dispersion of refractoriness and conduction heterogeneities are increased and are thought to be the causes of reentry and wavebreaks (El-Sherif et al., 1991; Janse and Wit, 1989; Restivo et al., 1990). Even though the heterogeneities are fixed in these hearts, arrhythmias still occurs in an unpredictable manner, indicating that dynamical changes in the triggers or substrates or both are needed. These changes can be caused by random fluctuations (such as random opening and closing of ion channels or emotion, etc.), or nonlinear dynamics arising from certain bifurcations, such as chaos, or by the interactions of random fluctuations and nonlinear dynamics. The roles of dynamical chaos in the genesis of human arrhythmias can be speculated as follows. First, chaos may play an important role in the degeneration of VT to VF in both structurally normal and abnormal hearts. Once VT is formed in the heart, either due to a reentry or a focus, its fast heart rate can drive the tissue into chaos to cause large dispersion of refractoriness and thus wavebreaks, giving rise to VF. Second, chaos may play an important role in arrhythmogenesis in structurally normal hearts, such as in patients with long QT syndromes (Roden, 2008; Schwartz, 2006) or catecholaminergic polymorphic VT (Napolitano and Priori, 2007). In these patients, arrhythmias may occur at fast heart rates caused by exercise-induced sympathetic activation or at slow heart rates during sleep or rest, both are associated with afterdepolarizations. Since these hearts are structurally normal, the pre-existing heterogeneities may not be large enough, regional synchronization of chaotic EADs may interact with the pre-existing heterogeneities to promote both the triggers and substrates for arrhythmogenesis in these diseased hearts.

Although it is difficult to directly demonstrate the roles of chaos in arrhythmogenesis in the human heart, the studies of computer simulation and animal experiments on the effects of chaos on genesis and maintenance of arrhythmias can provide insight into the mechanisms of the diseases as well as therapeutic strategies.

Acknowledgments

This work is supported by National Institute of Health, NHLBI P01 HL078931.

References

Akar FG, Rosenbaum DS. Transmural electrophysiological heterogeneities underlying arrhythmogenesis in heart failure. Circ Res. 2003; 93:638–645. [PubMed: 12933704]

Akar FG, Yan GX, Antzelevitch C, Rosenbaum DS. Unique topographical distribution of M cells underlies reentrant mechanism of torsade de pointes in the long-QT syndrome. Circulation. 2002; 105:1247–1253. [PubMed: 11889021]

Amino M, Yamazaki M, Nakagawa H, Honjo H, Okuno Y, Yoshioka K, Tanabe T, Yasui K, Lee JK, Horiba M, Kamiya K, Kodama I. Combined effects of nifekalant and lidocaine on the spiral-type re-entry in a perfused 2-dimensional layer of rabbit ventricular myocardium. Circ J. 2005; 69:576–584. [PubMed: 15849445]

Antzelevitch C, Sicouri S, Litovsky SH, Lukas A, Krishnan SC, Di Diego JM, Gintant GA, Liu DW. Heterogeneity within the ventricular wall. Electrophysiology and pharmacology of epicardial, endocardial, and M cells. Circ. Res. 1991; 69:1427–1449. [PubMed: 1659499]

Asano Y, Davidenko JM, Baxter WT, Gray RA, Jalife J. Optical mapping of drug-induced polymorphic arrhythmias and torsade de pointes in the isolated rabbit heart. J. Am. Coll. Cardiol. 1997; 29:831–842. [PubMed: 9091531]

Banville I, Gray RA. Effect of action potential duration and conduction velocity restitution and their spatial dispersion on alternans and the stability of arrhythmias. J. Cardiovasc. Electrophysiol. 2002; 13:1141–1149. [PubMed: 12475106]

Bar M, Eiswirth M. Turbulence due to spiral breakup in a continuous excitable medium. Phys.Rev.E. 1993; 48:R1635–R1637.

Beeler GW, Reuter H. Reconstruction of the action potential of ventricular myocardial fibres. J. Physiol. (Lond). 1977; 268:177–210. [PubMed: 874889]

Cao JM, Qu Z, Kim YH, Wu TJ, Garfinkel A, Weiss JN, Karagueuzian HS, Chen PS. Spatiotemporal heterogeneity in the induction of ventricular fibrillation by rapid pacing: importance of cardiac restitution properties. Circ. Res. 1999; 84:1318–1331. [PubMed: 10364570]

Chen P-S, Wolf PD, Dixon EG, Danieley ND, Frazier DW, Smith WM, Ideker RE. Mechanism of ventricular vulnerability to single premature stimuli in open chest dogs. Circ. Res. 1988; 62:1191–1209. [PubMed: 2454762]

Chen PS, Wu TJ, Ting CT, Karagueuzian HS, Garfinkel A, Lin SF, Weiss JN. A tale of two fibrillations. Circulation. 2003; 108:2298–2303. [PubMed: 14609997]

Chialvo DR, Gilmour RF, Jalife J. Low dimensional chaos in cardiac tissue. Nature. 1990a; 343:653–657. [PubMed: 2304537]

Chialvo DR, Michaels DC, Jalife J. Supernomal excitability as a mechanism of chaotic dynamics of activation in cardiac Purkinje fibers. Circ. Res. 1990b; 66:525–545. [PubMed: 2297816]

Choi BR, Burton F, Salama G. Cytosolic Ca^{2+} triggers early afterdepolarizations and Torsade de Pointes in rabbit hearts with type 2 long QT syndrome. J. Physiol. 2002; 543:615–631. [PubMed: 12205194]

Chugh SS, Kelly KL, Titus JL. Sudden cardiac death with apparently normal heart. Circulation. 2000; 102:649–654. [PubMed: 10931805]

Clayton RH, Murray A, Higham PD, Campbell RW. Self-terminating ventricular tachyarrhythmias--a diagnostic dilemma? Lancet. 1993; 341:93–95. [PubMed: 8093413]

Comtois P, Vinet A, Nattel S. Wave block formation in homogeneous excitable media following premature excitations: dependence on restitution relations. Phys. Rev. E. 2005; 72:031919.

El-Sherif N, Gough WB, Restivo M. Reentrant ventricular arrhythmias in the late myocardial infarction period: Mechanism by which a short-long-short cardiac sequence facilitates the induction of reentry. Circulation. 1991; 83:268–278. [PubMed: 1984885]

Fenton FH, Cherry EM, Hastings HM, Evans SJ. Multiple mechanisms of spiral wave breakup in a model of cardiac electrical activity. Chaos. 2002; 12:852–892. [PubMed: 12779613]

Franz MR, Swerdlow CD, Liem LB, Schaefer J. Cycle length dependence of human action potential duration in vivo: Effects of single extrastimuli, sudden sustained rate acceleration and deceleration, and different steady-state frequencies. J. Clin. Invest. 1988; 82:972–979. [PubMed: 3417875]

Garfinkel A, Kim YH, Voroshilovsky O, Qu Z, Kil JR, Lee MH, Karagueuzian HS, Weiss JN, Chen PS. Preventing ventricular fibrillation by flattening cardiac restitution. Proc. Natl. Acad. Sci. USA. 2000; 97:6061–6066. [PubMed: 10811880]

Garfinkel A, Spano ML, Ditto WL, Weiss JN. Controlling cardiac chaos. Science. 1992; 257:1230–1235. [PubMed: 1519060]

Garrey W. The nature of fibrillatory contraction of the heart: its relation to tissue mass and form. Am. J. Physiol. 1914; 33:397–414.

Gilmour RF Jr, Moise NS. Triggered activity as a mechanism for inherited ventricular arrhythmias in German shepherd Dogs. J. Am. Coll. Cardiol. 1996; 27:1526–1533. [PubMed: 8626969]

Glass L. Multistable spatiotemporal patterns of cardiac activity. Proc. Natl. Acad. Sci. U S A. 2005; 102:10409–10410. [PubMed: 16027355]

Goldhaber JI, Xie LH, Duong T, Motter C, Khuu K, Weiss JN. Action potential duration restitution and alternans in rabbit ventricular myocytes: the key role of intracellular calcium cycling. Circ. Res. 2005; 96:459–466. [PubMed: 15662034]

Goy JJ, Maendly R, Grbic M, Finci L, Sigwart U. Cardioversion with flecainide in patients with atrial fibrillation of recent onset. Eur. J. Clin. Pharmacol. 1985; 27:737–738. [PubMed: 3987780]

Guevara MR, Glass L. Phase locking, period doubling bifurcations and chaos in a mathematical model of a periodically driven oscillator: a theory for the entrainment of biological oscillators and the generation of cardiac dysrhythmias. J. Math. Biol. 1982; 14:1–23. [PubMed: 7077182]

Guevara MR, Glass L, Shrier A. Phase locking, period-doubling bifurcations, and irregular dynamics in periodically stimulated cardiac cells. Science. 1981; 214:1350–1353. [PubMed: 7313693]

Guevara MR, Ward G, Shrier A, Glass L. Electrical alternans and period doubling bifurcations. IEEE Comp. Cardiol. 1984; 562:167–170.

Hastings HM, Fenton FH, Evans SJ, Hotomaroglu O, Geetha J, Gittelson K, Nilson J, Garfinkel A. Alternans and the onset of ventricular fibrillation. Phys. Rev. E. 2000; 62:4043–4048.

Hilborn RC. Sea gulls, butterflies, and grasshoppers: A brief history of the butterfly effect in nonlinear dynamics. Am. J. Phys. 2004; 72:425–427.

Hwang C, Fan W, Chen P-S. Protective zones and the mechanisms of ventricular defibrillation. Am. J. Physiol. 1996; 271:H1491–H1497. [PubMed: 8897944]

Jalife J, Berenfeld O, Mansour M. Mother rotors and fibrillatory conduction: a mechanism of atrial fibrillation. Cardiovasc. Res. 2002; 54:204–216. [PubMed: 12062327]

Janse MJ. Focus, reentry, or "focal" reentry? Am. J. Physiol. 2007; 292:H2561–H2562.

Janse MJ, Wit AL. Electrophysiological mechanisms of ventricular arrhythmias resulting from myocardial ischemia and infarction. Physiol. Rev. 1989; 69:1046–1169.

Kim M-Y, Aguilar M, Hodge A, Vigmond E, Shrier A, Glass L. Stochastic and Spatial Influences on Drug-Induced Bifurcations in Cardiac Tissue Culture. Phys. Rev. Lett. 2009; 103:058101. [PubMed: 19792536]

Koller ML, Riccio ML, Gilmour RF Jr. Dynamic restitution of action potential duration during electrical alternans and ventricular fibrillation. Am. J. Physiol. 1998; 275:H1635–H1642. [PubMed: 9815071]

Laurita KR, Girouard SD, Rosenbaum DS. Modulation of ventricular repolarization by a premature stimulus. Role of epicardial dispersion of repolarization kinetics demonstrated by optical mapping of the intact guinea pig heart. Circ. Res. 1996; 79:493–503. [PubMed: 8781482]

Lerma C, Lee CF, Glass L, Goldberger AL. The rule of bigeminy revisited: analysis in sudden cardiac death syndrome. J. Electrocardiol. 2007; 40:78–88. [PubMed: 17069837]

Lewis TJ, Guevara MR. Chaotic dynamics in an ionic model of the propagated cardiac action potential. J. Theor. Biol. 1990; 146:407–432. [PubMed: 2259213]

Li GR, Lau CP, Ducharme A, Tardif JC, Nattel S. Transmural action potential and ionic current remodeling in ventricles of failing canine hearts. Am. J. Physiol. 2002; 283:H1031–H1041.

Lopshire JC, Zipes DP. Sudden Cardiac Death: Better Understanding of Risks, Mechanisms, and Treatment. Circulation. 2006; 114:1134–1136. [PubMed: 16966594]

Lorenz, EN. The Essence of Chaos. Seattle: University of Washington Press; 1994.

Mahajan A, Shiferaw Y, Sato D, Baher A, Olcese R, Xie L-H, Yang M-J, Chen P-S, Restrepo JG, Karma A, Garfinkel A, Qu Z, Weiss JN. A rabbit ventricular action potential model replicating cardiac dynamics at rapid heart rates. Biophys. J. 2008; 94:392–410. [PubMed: 18160660]

Manoach M, Varon D, Neuman M, Netz H. Spontaneous termination and initiation of ventricular fibrillation as a function of heart size, age, autonomic autoregulation, and drugs: a comparative study on different species of different age. Heart Vessels Suppl. 1987; 2:56–68. [PubMed: 3329649]

May RM. Simple mathematical models with very complicated dynamics. Nature. 1976; 261:459–467. [PubMed: 934280]

Moe GK. On the multiple wavelet hypothesis of atrial fibrillation. Arch. Int. Pharmacodyn. Ther. 1982; 14:183–188.

Moe GK, Rheinboldt WC, Abildskov JA. A computer model of atrial fibrillation. Am.Heart J. 1964; 67:200–220. [PubMed: 14118488]

Naccarelli GV, Wolbrette DL, Khan M, Bhatta L, Hynes J, Samii S, Luck J. Old and new antiarrhythmic drugs for converting and maintaining sinus rhythm in atrial fibrillation: comparative efficacy and results of trials. Am. J. Cardiol. 2003; 91:15D–26D.

Napolitano C, Priori SG. Diagnosis and treatment of catecholaminergic polymorphic ventricular tachycardia. Heart Rhythm. 2007; 4:675–678. [PubMed: 17467641]

Nolasco JB, Dahlen RW. A graphic method for the study of alternation in cardiac action potentials. J. Appl. Physiol. 1968; 25:191–196. [PubMed: 5666097]

Otani NF. Theory of action potential wave block at-a-distance in the heart. Phys. Rev. E. 2007; 75:021910–021917.

Otani NF, Li M, Gilmour RF Jr. What can nonlinear dynamics teach us about the development of ventricular tachycardia/ventricular fibrillation? Heart Rhythm. 2005; 2:1261–1263. [PubMed: 16253919]

Panfilov AV, Holden AV. Spatiotemporal irregularity in a two-dimensional model of cardiac tissue. Int. J. Bif. & Chaos. 1991; 1:219–225.

Pastore JM, Girouard SD, Laurita KR, Akar FG, Rosenbaum DS. Mechanism linking T-wave alternans to the genesis of cardiac fibrillation. Circulation. 1999; 99:1385–1394. [PubMed: 10077525]

Pecora LM, Carroll TL. Synchronization in chaotic systems. Phys. Rev. Lett. 1990; 64:821–824. [PubMed: 10042089]

Pecora LM, Carroll TL, Johnson GA, Mar DJ, Heagy JF. Fundamentals of synchronization in chaotic systems, concepts, and applications. Chaos. 1997; 7:520–543. [PubMed: 12779679]

Qu Z. Dynamical effects of diffusive cell coupling on cardiac excitation and propagation: a simulation study. Am. J. Physiol. 2004; 287:H2803–H2812.

Qu Z. Critical mass hypothesis revisited: role of dynamical wave stability in spontaneous termination of cardiac fibrillation. Am. J. Physiol. 2006; 290:H255–H263.

Qu, Z.; Garfinkel, A. Nonlinear dynamics of excitation and propagation in cardiac muscle. In: Zipes, DP.; Jalife, J., editors. Cardiac Electrophysiology: From Cell to Bedside. Philadelphia: Saunders; 2004. p. 327-335.

Qu Z, Garfinkel A, Chen PS, Weiss JN. Mechanisms of discordant alternans and induction of reentry in simulated cardiac tissue. Circulation. 2000a; 102:1664–1670. [PubMed: 11015345]

Qu Z, Garfinkel A, Weiss JN. Vulnerable window for conduction block in a one-dimensional cable of cardiac cells, 2: Multiple extrasystoles. Biophys. J. 2006a; 91:805–815. [PubMed: 16679366]

Qu Z, Garfinkel A, Weiss JN. Vulnerable window for conduction block in a one-dimensional cable of cardiac cells, 1: Single extrasystoles. Biophys. J. 2006b; 91:793–804. [PubMed: 16679367]

Qu Z, Shiferaw Y, Weiss JN. Nonlinear dynamics of cardiac excitation-contraction coupling: an iterated map study. Phys. Rev. E. 2007; 75:011927.

Qu Z, Weiss JN. Effects of Na^+ and K^+ channel blockade on vulnerability to and termination of fibrillation in simulated normal cardiac tissue. Am. J. Physiol. 2005; 289:H1692–H1701.

Qu Z, Weiss JN. Dynamics and cardiac arrhythmias. J. Cardiovasc. Electrophysiol. 2006; 17:1042–1049. [PubMed: 16899089]

Qu Z, Weiss JN, Garfinkel A. Cardiac electrical restitution properties and the stability of reentrant spiral waves: A simulation study. Am. J. Physiol. 1999; 276:H269–H283. [PubMed: 9887041]

Qu Z, Weiss JN, Garfinkel A. From local to global spatiotemporal chaos in a cardiac tissue model. Phys. Rev. E. 2000b; 61:727–732.

Qu Z, Xie F, Garfinkel A, Weiss JN. Origins of spiral wave meander and breakup in a two-dimensional cardiac tissue model. Ann. Biomed. Eng. 2000c; 28:755–771. [PubMed: 11016413]

Restivo M, Caref EB, Kozhevnikov DO, El-Sherif N. Spatial dispersion of repolarization is a key factor in the arrhythmogenicity of long QT syndrome. J. Cardiovasc. Electrophysiol. 2004; 15:323–331. [PubMed: 15030424]

Restivo M, Gough W, El-Sherif N. Ventricular arrhythmias in the subacute myocardial infarction period. High-resolution activation and refractory patterns of reentrant rhythms. Circ. Res. 1990; 66:1310–1327. [PubMed: 2335029]

Riccio ML, Koller ML, Gilmour RF Jr. Electrical restitution and spatiotemporal organization during ventricular fibrillation. Circ. Res. 1999; 84:955–963. [PubMed: 10222343]

Roden DM. Long-QT Syndrome. N. Engl. J. Med. 2008; 358:169–176. [PubMed: 18184962]

Sato D, Xie L-H, Nguyen TP, Weiss JN, Qu Z. Irregularly Appearing Early Afterdepolarizations in Cardiac Myocytes: Random Fluctuations or Dynamical Chaos? Biophys. J. 2010; 99 (in press).

Sato D, Xie LH, Sovari AA, Tran DX, Morita N, Xie F, Karagueuzian H, Garfinkel A, Weiss JN, Qu Z. Synchronization of chaotic early afterdepolarizations in the genesis of cardiac arrhythmias. Proc. Natl. Acad. Sci. U S A. 2009; 106:2983–2988. [PubMed: 19218447]

Schwartz PJ. The congenital long QT syndromes from genotype to phenotype: clinical implications. J. Intern. Med. 2006; 259:39–47. [PubMed: 16336512]

Song Y, Thedford S, Lerman BB, Belardinelli L. Adenosine-sensitive afterdepolarizations and triggered activity in guinea pig ventricular myocytes. Circ. Res. 1992; 70:743–753. [PubMed: 1551200]

Strogatz, SH. Studies in nonlinearity. Westview Press; 2000. Nonlinear dynamics and Chaos: with applications to physics, biology, chemistry, and engineering; p. xip. 498

Tanskanen AJ, Greenstein JL, O'Rourke B, Winslow RL. The role of stochastic and modal gating of cardiac L-type Ca^{2+} channels on early after-depolarizations. Biophys. J. 2005; 88:85–95. [PubMed: 15501946]

Tran DX, Sato D, Yochelis A, Weiss JN, Garfinkel A, Qu Z. Bifurcation and chaos in a model of cardiac early afterdepolarizations. Phys. Rev. Lett. 2009; 102:258103. [PubMed: 19659123]

Waldo AL, Wit AL. Mechanisms of cardiac arrhythmias. Lancet. 1993; 341:1189–1193. [PubMed: 8098085]

Wang S, Xie Y, Qu Z. Coupled iterated map models of action potential dynamics in a one-dimensional cable of coupled cardiac cells. New J. Phys. 2007; 10:055001.

Watanabe M, Otani NF, Gilmour RF. Biphasic restitution of action potential duration and complex dynamics in ventricular myocardium. Circ. Res. 1995; 76:915–921. [PubMed: 7729010]

Weiss JN, Karma A, Shiferaw Y, Chen PS, Garfinkel A, Qu Z. From pulsus to pulseless: the saga of cardiac alternans. Circ. Res. 2006; 98:1244–1253. [PubMed: 16728670]

Weiss JN, Qu Z, Chen PS, Lin SF, Karagueuzian HS, Hayashi H, Garfinkel A, Karma A. The dynamics of cardiac fibrillation. Circulation. 2005; 112:1232–1240. [PubMed: 16116073]

Wijffels M, Dorland R, Mast F, Allessie MA. Widening of the excitable gap during pharmacological cardioversion of atrial fibrillation in the goat - Effects of cibenzoline, hydroquinidine, flecainide, and d-sotalol. Circulation. 2000; 102:260–267. [PubMed: 10889140]

Wijffels M, Kirchhof C, Dorland R, Allessie MA. Atrial Fibrillation Begets Atrial Fibrillation - a Study in Awake Chronically Instrumented Goats. Circulation. 1995; 92:1954–1968. [PubMed: 7671380]

Winfree AT. Sudden cardiac death: a problem in topology. Sci. Am. 1983; 248:144–149. 152–157, 160–161. [PubMed: 6857229]

Wu TJ, Kerwin WF, Hwang C, Peter CT, Chen PS. Atrial fibrillation: focal activity, re-entry, or both? Heart Rhythm. 2004; 1:117–120. [PubMed: 15851128]

Wu TJ, Lin SF, Weiss JN, Ting CT, Chen PS. Two types of ventricular fibrillation in isolated rabbit hearts - Importance of excitability and action potential duration restitution. Circulation. 2002; 106:1859–1866. [PubMed: 12356642]

Xie Y, Hu G, Sato D, Weiss JN, Garfinkel A, Qu Z. Dispersion of refractoriness and induction of reentry due to chaos synchronization in a model of cardiac tissue. Phys. Rev. Lett. 2007; 99:118101. [PubMed: 17930473]

Yamazaki M, Honjo H, Nakagawa H, Ishiguro YS, Okuno Y, Amino M, Sakuma I, Kamiya K, Kodama I. Mechanisms of destabilization and early termination of spiral wave reentry in the ventricle by a class III antiarrhythmic agent, nifekalant. Am. J. Physiol. 2007; 292:H539–H548.

Zipes DP, Wellens HJ. Sudden cardiac death. Circulation. 1998; 98:2334–2351. [PubMed: 9826323]

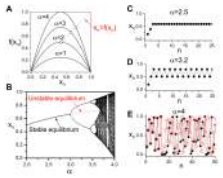

Figure 1. Chaos and sensitive dependence on initial conditions

A. Plots of $f(x_n)$ for different α. Open circles are the equilibrium states which are the intersections of the parabolae (solid lines) and the diagonal line [dashed line, $x_n=f(x_n)$]. **B**. Bifurcation diagram showing x_n versus α. For each value of α, Eq.2 is iterated 300 steps with the first 100 values of x_n (n=1 to 100) dropped and the rest 200 values plotted. The dashed line is the unstable equilibrium state. **C**. x_n versus n for α=2.5. **D**. x_n versus n for α=2.5. **E**. x_n versus n for α=4 with an initial value x_1=0.2 (solid circles) and with an initial value slightly different from 0.2, i.e., x_1=0.20001 (open circles).

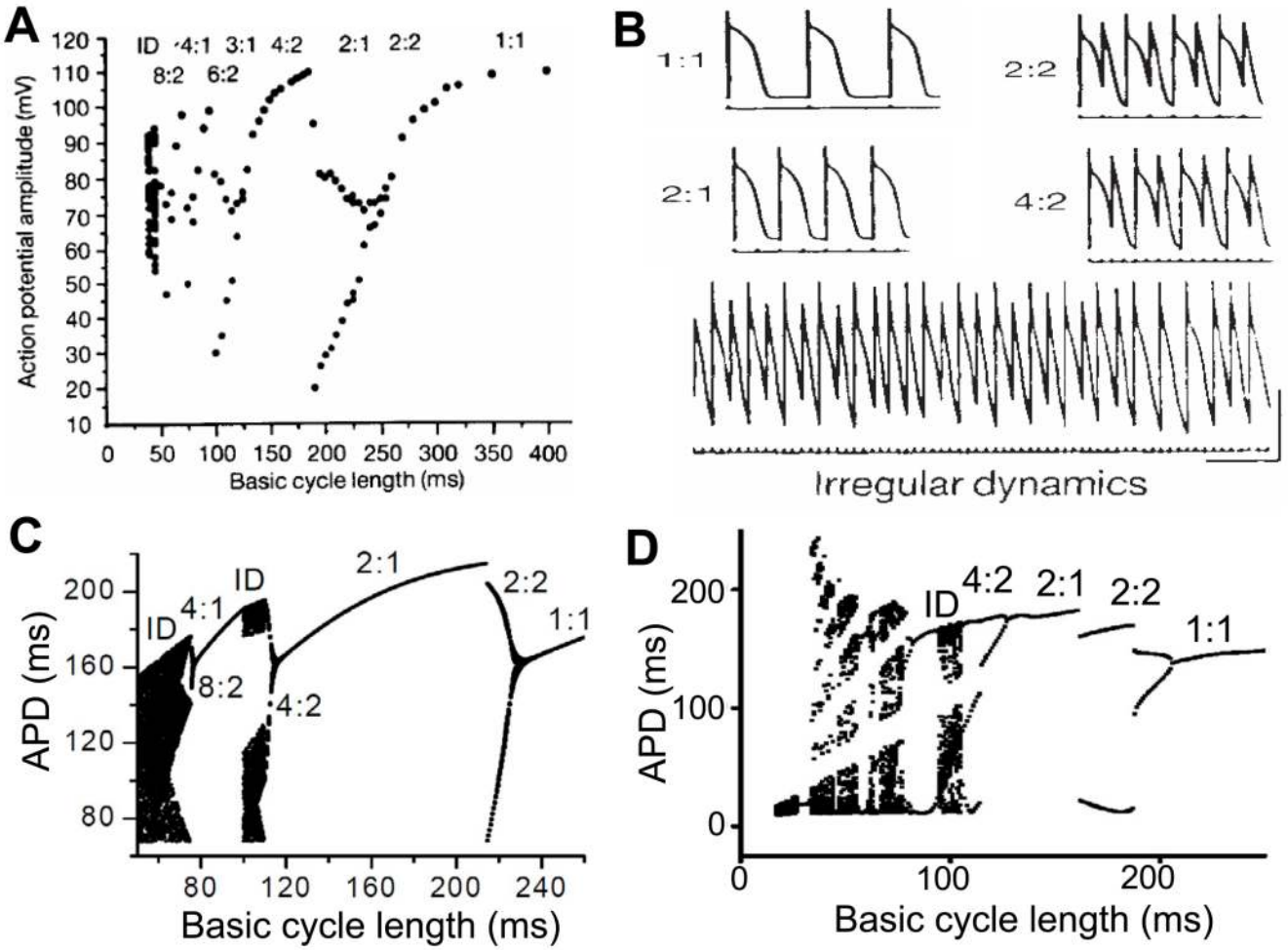

Figure 2. Cardiac chaos

A. Bifurcation diagram showing the relationship between the basic cycle length of pacing and beat-to-beat action potential amplitudes in a sheep cardiac Purkinje fiber (Chialvo et al., 1990a). The observed bifurcation sequence is: 1:1 → 2:2 → 2:1 → 4:2 → 3:1 → 6:2 → 4:1 → 8:2 → ID. "n:m" indicates that *n* stimuli elicit *m* different action potentials, which repeat periodically, e.g., "4:2" means that for each 4 stimuli, 2 action potentials with different morphologies are elicited, which is simply APD alternans. "ID" stands for irregular dynamics or dynamical chaos. **B**. Action potential recordings from a dog cardiac Purkinje fiber at different basic cycle length, showing 1:1, 2:2, 2:1, 4:2, and irregular dynamics (Chialvo et al., 1990a). **C**. Bifurcation diagram showing APD versus basic cycle length from an iterated map. The bifurcation sequence shows: 1:1 → 2:2 → 2:1 → 4:2 → ID → 4:1 → 8:2 → ID. The bifurcation diagram is generated using iterated map Eq.3 with the APD restitution function: $APD_{n+1} = f(DI_n) = 220 - 180e^{-DI_n/60}$, and the relation: $DI_n = PCL - APD_n$. For each PCL, the first 40 APDs are discarded and the next 100 APDs are plotted. In the alternans (2:2) regime, there are only two APD values though 100 APDs are plotted, however, in the chaotic regime, the values of the 100 APDs are all different, resulting in scattered plots. **D**. Bifurcation diagram showing APD versus basic cycle length from a computer simulation using the Beeler-Reuter action potential model (Xie et al., 2007).

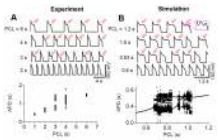

Figure 3. Chaotic EAD dynamics in cardiac myocytes (Sato et al., 2009)

A and **B**. Voltage recordings and bifurcation diagrams (APD vs. PCL) from a paced rabbit ventricular myocyte exposed to 1 mM H_2O_2 (A), and a ventricular action potential model (B), illustrating that irregular EADs occur only at intermediate PCLs. Red arrows indicate EADs.

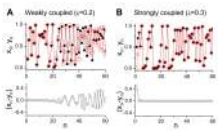

Figure 4. Chaos synchronization in diffusively coupled Logistic maps

A. Top: x_n (solid circles) and y_n (open circles) versus n. Bottom: The difference ($x_n - y_n$) of x_n and y_n versus n. ε=0.2. **B**. Same as A but for ε=0.3.

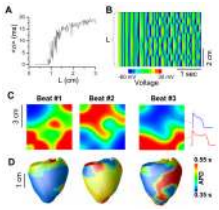

Figure 5. Chaos synchronization in cardiac tissue

A and **B**. Chaos synchronization in a 1D homogeneous cable of coupled myocytes under rapid pacing (Xie et al., 2007). Panel A shows the average standard deviation (<σ>) of voltage versus the cable length L. <σ> is defined as:

$$<\sigma>=\lim_{T\to\infty}\frac{1}{T-T_0}\int_{T_0}^{T}dt\sqrt{\int_0^L[V(x,t)-\overline{V}(t)]^2dx/L}$$

, where $\overline{V}(t)$ is the average voltage over the whole cable at time t, T_0 is a time after the transient, and L is the length of the cable. Synchronization therefore occurs when <σ> approaches zero. All myocytes are identically paced with PCL=100 ms. The myocytes are modeled by the Beeler-Reuter model (Beeler and Reuter, 1977) with modifications (Xie et al., 2007), which exhibits a bifurcation diagram similar to the ones shown in Fig.2. Panel B shows the time-space plot of voltage for L=6 cm for the same 1D cable as in A. **C** and **D**. Chaos synchronization in cardiac tissue due to EAD chaos at slow pacing (Sato et al., 2009). Panel C shows APD distributions for three consecutive beats in homogeneous 2D tissue (4.5 cm × 4.5 cm) with stimuli applied uniformly at the left edge of the tissue. Islands of long APD (with EADs) surrounded by regions with short APD (without EADs) developed as a result of the spatial instabilities. Panel D shows APD distributions for three consecutive beats in an anatomical rabbit ventricle model paced from a single site in the apex, illustrating similar islands of long APD.

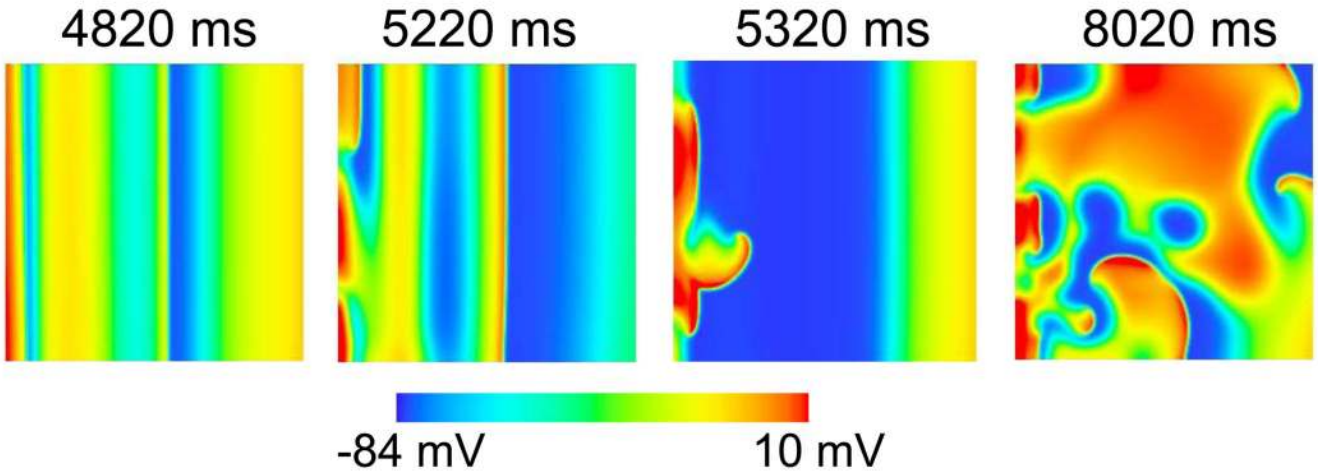

Figure 6. Reentry induction in homogeneous tissue (Xie et al., 2007)

Voltage snapshots showing reentry induction in a 7.5 cm × 7.5 cm homogeneous tissue with the modified Beeler-Reuter model and PCL=100 ms. Stimulation is applied in a narrow strip (0.3×7.5 cm^2) spanning the left border of the tissue, inducing planar waves propagating from left to right. Chaos desynchronization is first induced in the region around the pacing site, followed by local conduction block and eventually complex reentrant patterns.

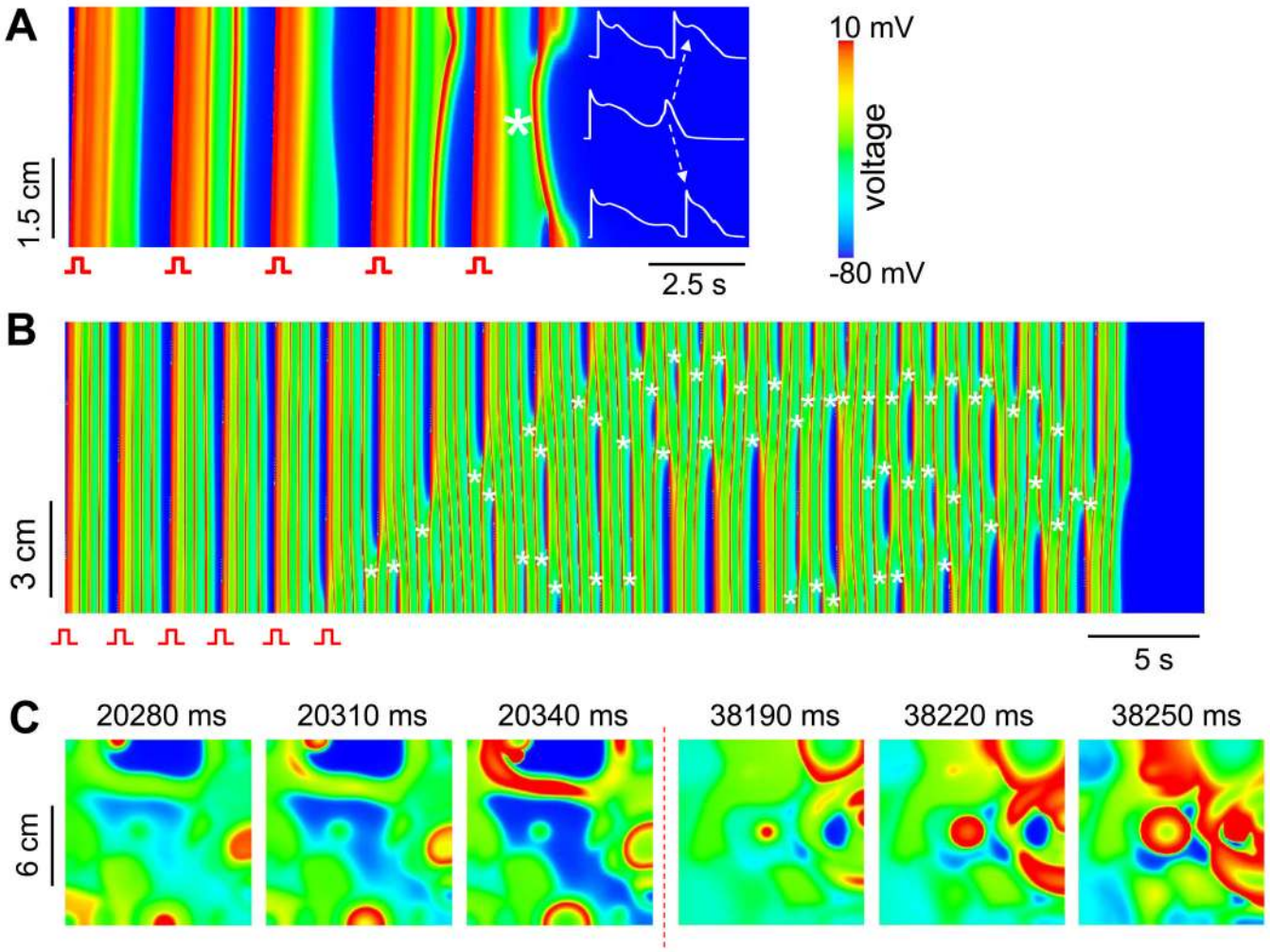

Figure 7. PVC formation in homogeneous tissue (Sato et al., 2009)

A. Space (y-axis) and time (x-axis) plot of voltage in a 1D cable paced at one end. A localized EAD (*) which forms at the center of the cable after the 5th paced beat (middle inset trace) propagates as a PVC towards both ends (top and bottom inset traces). **B**. Space (y-axis) and time (x-axis) plot of voltage in a 9 cm homogeneous 1D cable paced at one end for six beats (as indicated) showing the formation of multiple shifting foci (*) due to regional chaos synchronization. **C**. Voltage snapshots of two episodes (from 20280 ms to 20340 ms, and from 38190 ms to 38250 ms) of multiple shifting foci from a simulation in a 12 cm × 12 cm homogeneous 2D tissue.

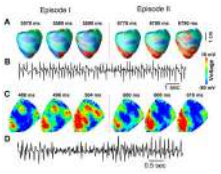

Figure 8. Multiple shifting foci resembling polymorphic VT (Sato et al., 2009)

A. Multiple EAD-induced shifting foci are shown in voltage snapshots on the epicardical surface of the anatomic rabbit ventricle model. Note that the positions of the foci in the two epochs (from 5570 ms to 5590 ms, and from 6770 ms to 6790 ms) have shifted to new locations. **B**. Pseudo-electrocardiogram of A, illustrating polymorphic VT resembling Torsade de pointes. **C**. Voltage snapshots on the epicardical surface of a rabbit heart during exposure to 0.2 mM H_2O_2, showing two episodes of multiple EAD-induced foci (from 488 ms to 504 ms with three foci, and from 600 ms to 608 ms with one focus) similar to the simulation in A. **D**. Pseudo-electrocardiogram of C, illustrating polymorphic VT resembling Torsade de Pointes.

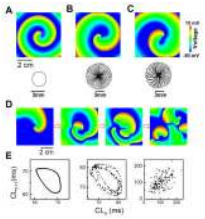

Figure 9. Spiral wave breakup leading to spatiotemporal chaos resembling VF (Qu et al., 2000c)

A–C. Voltage snapshot of a spiral wave and its tip trajectory for a stable (A); a quasiperiodically meandering (B), and chaotically meandering (C) spiral wave. **D**. Voltage snapshots showing a spiral wave breaks up into multiple spiral waves. **E**. Cycle length (CL), recorded from one of the tissue, at the present beat (CL_{n+1}) is plotted against the previous beat (CL_n), showing quasiperiodicity of the quasiperiodically meandering spiral wave (left) and chaos from the chaotically meandering spiral wave (middle) and spiral wave breakup (right).

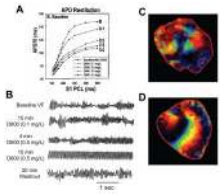

Figure 10. Experiments showing APD restitution dependent transitions from VF to VT and from VT to VF in the presence and absence of D600 in a rabbit heart (Wu et al., 2002)

A. APD restitution curves at different D600 concentrations, plotted as APD against pacing cycle length. **B**. Pseudo-ECGs showing baseline VF, transition from VF to VT at D600 concentration of 0.5 mg/L, and transition from VT to VF after the drug is washed out. **C**. A snapshot of optical signal during baseline VF showing multiple wavefronts. **D**. A snapshot of optical signal during VT showing a pair of stable spiral waves.

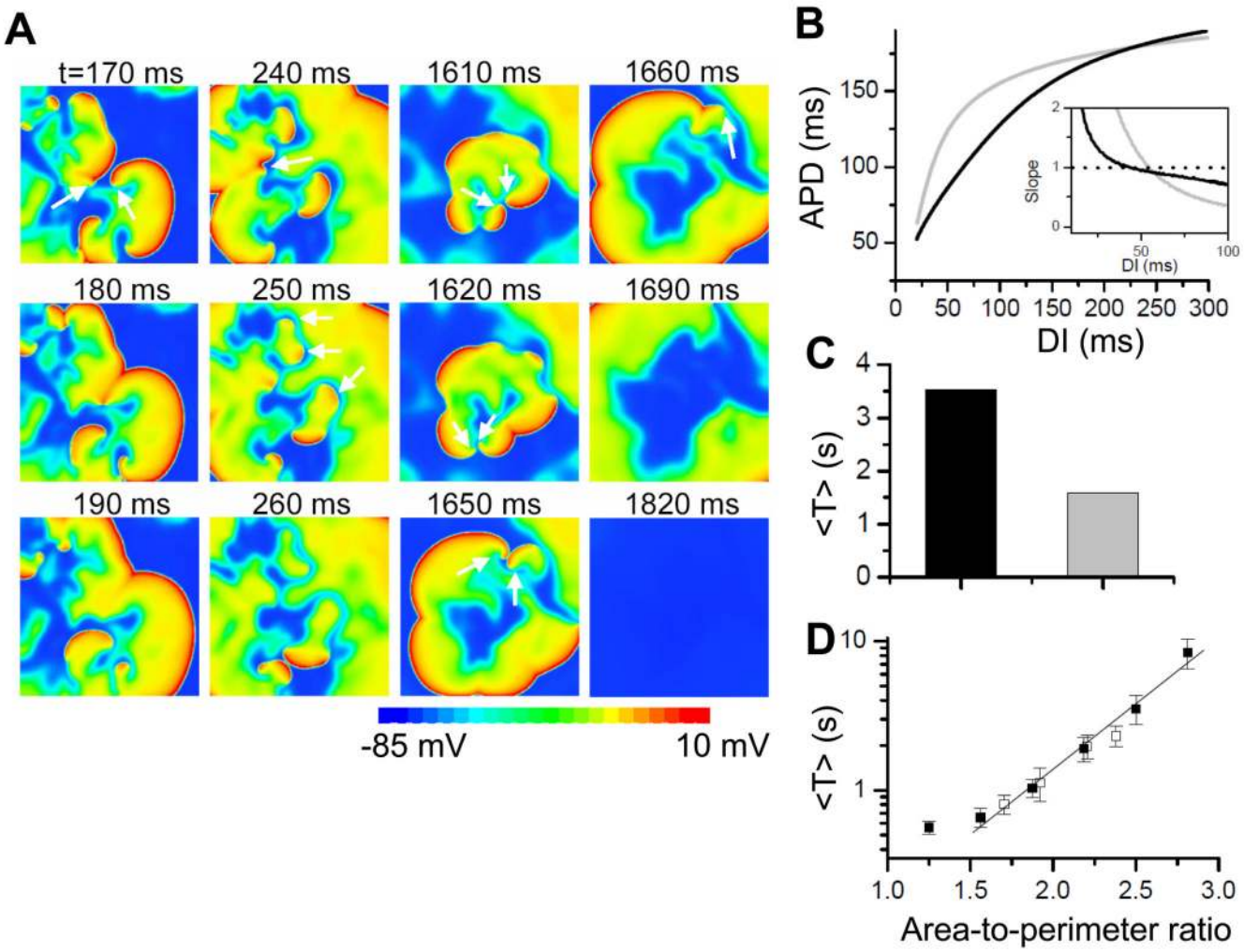

Figure 11. Chaos in termination of fibrillation (Qu, 2006)

A. Voltage snapshots showing self-termination of "multiple-wavelet" fibrillation from a simulation in a 10 × 10 cm^2 homogeneous tissue model. *Column 1* (170–190 ms): 2 spiral waves (arrows) at 170 ms collide at 180 ms and disappear at 190 ms. *Column 2* (240–260 ms): spiral waves (arrows) at 240 and 250 ms run into refractory tails of their previous waves and disappear at 260 ms. *Column 3* (1,610 –1,650 ms): spiral pairs (arrows) collide and disappear. *Column 4* (1,660 –1,820 ms): the only surviving spiral wave (arrow) moves off the tissue border, and the tissue becomes quiescent. **B**. Two APD restitution curves with different slopes. **C**. Average VF duration <T> for the two APD restitution curves in B. **D**. Average VF duration <T> versus the area-to-perimeter ratio from a square tissue (black) and a rectangular tissue (open).